Earth Moon Planets (2015) 115:1–21
DOI 10.1007/s11038-015-9462-1

First Lunar Flashes Observed from Morocco (ILIAD Network): Implications for Lunar Seismology

Mamoun Ait Moulay Larbi · Ahmed Daassou · David Baratoux · Sylvain Bouley · Zouhair Benkhaldoun · Mohamed Lazrek · Raphael Garcia · Francois Colas

Received: 24 May 2014 / Accepted: 16 February 2015 / Published online: 4 March 2015
© Springer Science+Business Media Dordrecht 2015

Abstract We report the detection of two transient luminous events recorded on the lunar surface on February 6, 2013, at 06:29:56.7 UT and April 14, 2013, 20:00:45.4 from the Atlas Golf Marrakech observatory in Morocco. Estimated visual magnitudes are 9.4 ± 0.2 and 7.7 ± 0.2. We show that these events have the typical characteristics of impact flashes generated by meteoroids impacting the lunar surface, despite proof using two different telescopes is not available. Assuming these events were lunar impact flashes, meteoroid masses are 0.3 ± 0.05 and 1.8 ± 0.3 kg, corresponding to diameters of 7–8 and 14–15 cm for a density of 1500 kg m^{-3}. The meteoroids would have produced craters of about 2.6 ± 0.3 and 4.4 ± 0.3 m in diameter. We then present a method based on the identification of lunar features illuminated by the Earthshine to determine the position of the flash. The method does not require any information about the observation geometry or lunar configuration. The coordinates are respectively 08.15° ± 0.15°S 59.1° ± 0.15°E and 26.81° ± 0.15°N 09.10° ± 0.15°W. Further improvement on the determination of the flash position is necessary for seismological applications. This studies demonstrates that permanent lunar impact flashes observation programs may be run in different parts of the globe using mid-sized telescopes. We call for the development of an international lunar

M. Ait Moulay Larbi (✉) · A. Daassou · Z. Benkhaldoun · M. Lazrek
Laboratoire de Physique des Hautes Energies et Astrophysique, FSSM, Université Cadi Ayyad, Av. Prince My Abdallah, BP 2390 Marrakech, Marocco
e-mail: elmamoun.aitmylarbi@edu.uca.ma

M. Ait Moulay Larbi · D. Baratoux
UPS-OMP, GET, Université de Toulouse, Toulouse, France

S. Bouley
GEOPS, UMR8148, Université Paris-Sud, 91405 Orsay Cedex, France

S. Bouley · F. Colas
Institut de Mécanique Céleste et de Calcul des Ephémérides, Observatoire de Paris, 75014 Paris, France

R. Garcia
Institut Supérieur de l'Aéronautique et de l'Espace (ISAE), Toulouse, France

impact astronomical detection networks that would represent an opportunity for scientific and cultural developments in countries where astronomy is under-represented.

Keywords Meteoroids · Impact flash · Crater · Moon

1 Introduction

Significant discoveries and progresses in understanding planetary evolution are largely based on our capacity to determine a precise chronological sequence of geological events affecting the solid bodies on our solar system. This statement has been recently well illustrated with, for instance, the findings and interpretations of major transitions affecting igneous rocks or their alteration products at the surface of Mars (Bibring et al. 2006; Poulet et al. 2009; Baratoux et al. 2013), the unexpected occurrences of young ages at the surface of Moon and Mars (Neukum et al. 2004; Vaucher et al. 2009; Hiesinger et al. 2010), or the violent collisional history of Vesta (Marchi et al. 2012) including the $\sim$1 Ga old event responsible for the formation of the Rheasilvia basin. With the exception of the Earth, chronological scales of all rocky bodies rely on the extrapolations of relationships between crater densities at the surface of the Moon and exposure time to the meteoritic bombardment inferred from the geochronological analysis of Apollo samples (Hartmann 2005). Given the inferred age-distribution of Apollo samples, variation of the impact flux with time, in particular over the last 3 Ga, is poorly known (Quantin et al. 2007; Marchi et al. 2009). It has also been shown that the cratering rate varies with position, as a consequence of the non-isotropic distribution of orbital parameters of impactors and of the orbital parameters of the object (Le Feuvre and Wieczorek 2008, 2011). The cratering rate (assumed to be constant over the last 3 Ga) would compare within one order of magnitude with the impact flux inferred from detonations associated with bolides entering the Earth atmosphere, or with the flux inferred from impacts recorded by the Apollo seismometers (Brown et al. 2002; Ivanov 2006; Mimoun et al. 2012). However, these comparisons involve the use of empirical and poorly constrained scaling laws through which the various measured physical quantities such as crater diameter, seismic energy, or radiation may be related (Mimoun et al. 2012; Oberst et al. 2012).

The possibility to observe lunar flashes by using ground-based telescopes has appeared more than a decade ago (Rubio et al. 2000; Ortiz et al. 2000, 2006; Yanagisawa et al. 2006; Iye et al. 2007) and offers another new opportunity to document the present impact rate for kilogram-size meteoroids (Suggs et al. 2014). Mid-sized telescopes equipped with focal reducers and inexpensive video cameras are generally sufficient to monitor large meteoroids hitting the Moon (Oberst et al. 2012; Mousis and et al. 2013). These icy, rocky or stony meteoroids hit the Moon with velocities ranging from less than 10 km/s to more than 70 km/s. A fraction of the kinetic energy transferred to the lunar rocks is converted into radiation producing a transient and brief (typically less than 1 s) luminous event associated with heating of the target and formation of a plume involving during its expansion and cooling variable proportions of plasma and vapor phases, liquid droplets and hot solid particles (Yanagisawa et al. 2006; Melosh et al. 1993; Clark and Melosh 1996; Artemieva et al. 2001; Davis 2009; Bouley et al. 2012). The relative contribution of each phase to the thermal emission should evolve as a function of time. Plasma emission may dominate the early stages, and hot solid or liquid materials are expected to be dominant in the late stage of expansing and cooling of the plume. It has been actually argued that the typical duration of impact flashes is too long when compared with radiative transfer models in a plasma/vapor expanding plume (Bouley et al. 2012). It was also noted that the light curve may be approximated by that of a expanding cloud of liquid silicate droplets with a black body law and an effective temperature close to that of the liquid/vapor transition of silicates (Bouley et al. 2012; Yanagisawa and Kisaichi 2002).

The observation of lunar-meteoroids impact flashes is motivated in the context of projects for future lunar seismological networks (Mimoun et al. 2012). Impacts represent an important part of the catalogue of seismic events (Lognonné et al. 2009). The simultaneous monitoring from the ground of impact flashes opens the possibility to provide independent positions and times of the seismic source, leading to improvements in the determination of the crustal structure (Yamada et al. 2011). Such data becomes indispensable in the case of a one-seismometer mission. Other motivations are related to the exploration of the lunar atmosphere mission (e.g., LADEE—lunar atmosphere and dust environment explorer), or the search for new impact structures on the lunar surface (e.g., LROC—Lunar Reconnaissance Orbiter Camera), and the measure of the largest meteoroids within the principal annual meteoroid streams.

Permanent and automated monitoring stations exist only in North America and Spain (Suggs et al. 2014; Cooke et al. 2007; Madiedo et al. 2009, 2013). We therefore call for the development of an international project (ILIAD—international lunar impacts astronomical detection) with the objective to develop lunar impact flashes monitoring programs in several stations around the globe. Automated stations are certainly the best option when sufficient funding is available. At this stage, our observations are not yet automated and the time-consuming workload is the main limitation to our capabilities. Despite these difficulties, we report here the two first flashes detected in the frame of the project at the Atlas Golf Marrakech (AGM) observatory, respectively on the February 6, 2013, at 06:29:56.7 UT and April 14, 2013, 20:00:45.4 UT. We present the characteristics of these two impact flashes. In the context of the conceived future applications to lunar seismology, we developed and tested new strategies for the accurate determination of the coordinates of each impact. We also present an evaluation of the implications of the position uncertainties for seismological applications.

2 Observations and Analysis

2.1 Facilities Dedicated to the Observation of Impact Flashes in Morocco

The geographical coordinates of Moroccan stations are 7°52′52″W longitude and 31°12′32″N latitude (Oukaimden observatory) and 7°59′35″W longitude and 31°37′28″N latitude (AGM observatory). The instrumental setup consisted of two 355-mm diameter Schmidt-Cassegrain and a 200-mm f/10 telescopes (Fig. 1). The diameters of the telescopes are appropriate for such observations and large enough for the detection of events having visual magnitudes between 3 and 10. Impact flashes can only be detected during the lunar night (dark side of the lunar disk), therefore 10 nights of observations per lunar month must be dedicated to impact flash monitoring, 5 during the waxing crescent and 5 during the waning crescent.

The number of detections is proportional to the monitored surface of the non-illuminated fraction of the lunar disk, which depends on the field of view. For this reason, we use focal reducer systems, respectively 0.33× or 0.63× for the the 355-mm telescope and the 200-mm telescope, and C-mount spacers with adapters in front of the cameras. With these systems, the field of view can enclose between 30 and 70 % of the lunar disk. The actual

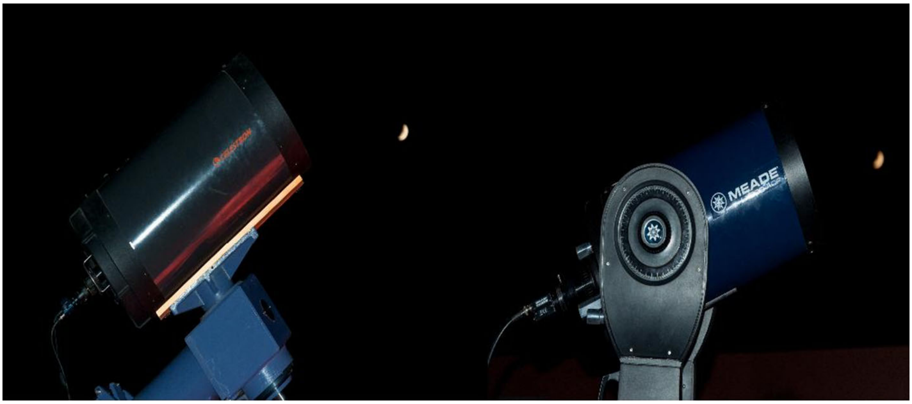

Fig. 1 Photographies of the two telescopes dedicated to impact flash monitoring during 10 nights/month in Marrakesh and Oukaimden observatoties

Table 1 Characteristics of equipments used during the observation of the flashes 1 and 2 (image resolution can be improved (in PAL mode) by choosing 720 x 576 rather than 640*480 pixels)

	Flash 1	Flash 2
Diameter (mm)	200	335
Initial focal length (mm)	2000	3910
Focal reducer system	0.63×	0.33×
Camera type	Watec 902H2	Watec 902H2
Camera sensor (pixels)	752 × 582	752 × 582
Pixels (µm)	8.6 × 8.3	8.6 × 8.3
Field of view (arc min')	14 × 10.5	19 × 14
Image dimension (pixels)	640 × 480	640 × 480
Approximate lunar surface monitored (km^2)	$\approx 1.8 \times 10^6$	$\approx 4 \times 10^6$
Resolution (km)	4 ± 1	5 ± 1
Time recording system	GPS-Time inseters	GPS-Time inserters

value depends on the distance between the camera sensor and the telescope which varies according to the length of the spacers and the adapters and the manner in which they are mounted. In practice, the observed surface of the Moon may be further limited by avoiding observations near the terminator in order to limit light diffusion from the illuminated fraction of the lunar disk.

Images are recorded using high-speed black-and-white CCD video cameras (Watec WAT-902H2 or WAT-120N , at 29.97 frames per second (NTSC) or 25 frames per second (PAL)). GPS time inserters are used to stamp time on every video frame with a precision of 0.001 ms. The video signal is then digitized and recorded to the hard-drive.

The LunarScan software (Gural 2007; Cudnik 2009) is used on recorded videos to perform an automated detections of transient events in the field of view. The automatically detected transient events are then manually examined to eliminate false detections and select those having the typical characteristics of impact flashes in terms of intensity, spatial extension and duration. The characteristics of our equipment are summarized in the Table 1.

2.2 Data Processing and Characteristics of Recorded Events

The characteristics and conditions of observations of two transient luminous events, recorded respectively on February 6, 2013, at 06:29:56.7 UT (flash 1) and April 14, 2013, at 20:00:45.4 UT (flash 2) are summarized here. Frames of two flashes are shown in Fig. 2. The February 6, 2013 flash (flash 1) was recorded using Watec 902H2 video camera attached to a 0.2 m f/10 telescope with a 0.63× focal reducer, following 5 h of monitoring during the nights of the 5 and 6 of February. The time of the detection corresponds to an observation made just before sunrise. The flash is seen in 2 video frames with a total duration greater than 80 ms. The second reported observation (flash 2) correspond to a series of monitoring sessions made from the 14th to the 17th April. 10 h of video frames were recorded during the 4 nights with a 355-mm telescope equipped with a 0.33× focal reducer. This flash was actually observed during the first 5 min of the first night of this series of observations, and no additional detections were reported on the 10 h long data record. The flash appears near the edge of the frame and was also detected automatically by LunarScan. It is seen in 5 video full-frames with a total duration greater than 200 ms. The intensity peaks on the second frame of the series (Fig. 3).

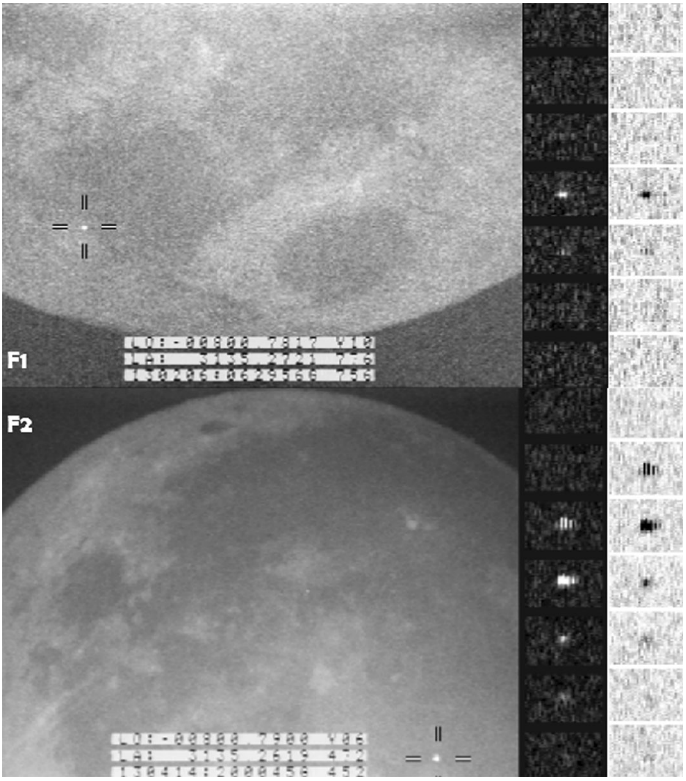

Fig. 2 Lunar impact flashes detected with LunarScan software (Gural 2007; Cudnik 2009) with a multi-frame subimage of the raw imagery for each event (in positive and negative). F1 (*up*): February 6, 2013 impact flash, F2 (*down*): April 14, 2013 impact flash

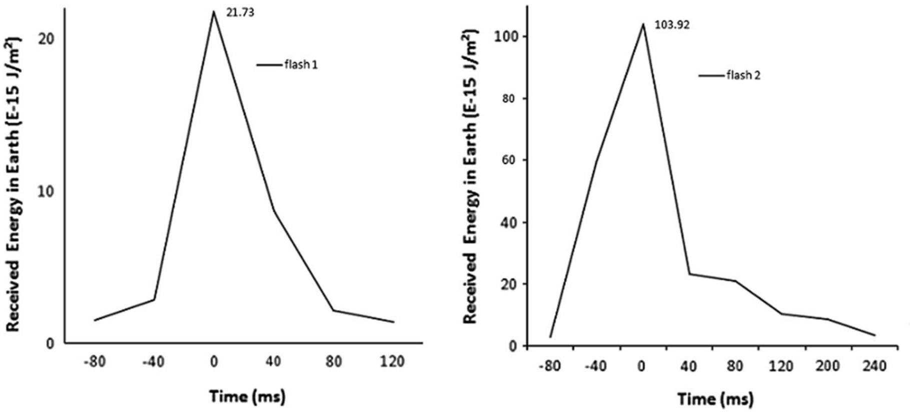

Fig. 3 (*Left*) Light curve of flash recorded on February 6, 2013. (*Right*) Light curve of flash recorded on April 14, 2013

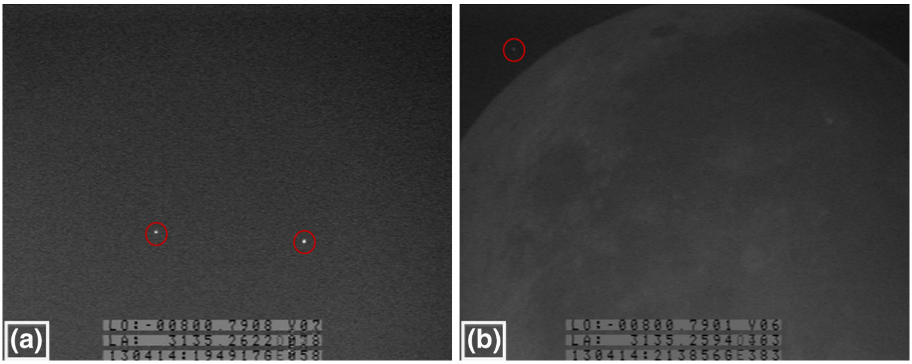

Fig. 4 Example of typical video frames of stars used to calibrate photometric measurements of flash detected on April 14, (frames before preprocessing). **a** HIP 22672 and HIP 22684 stars with visual magnitude of 8.7 and 9.4, this field was targeted at 10 arcmin north of the lunar disk, it was recorded 5 min before the start of observation and 10 min before the flash detection, **b** a 10 visual magnitude star appeared in the field of view just before moonset during the same night

Once identified, the frames containing the flash were extracted for photometric analysis. To calculate the flash magnitude in each frame we used the technique of aperture photometry, available under the IRAF software in Apphot package. We have checked our results with other processing software (Limovie, Iris). To achieve the best estimate of magnitude we prepare before the observation a list of the best reference stars (with known visual magnitude) that will pass near the lunar disk or that will appear occasionally in the field of view during the night of observation. In practice, if there was an insufficient number of stars that appears in the field of view during monitoring, it useful to record a short video to some reference stars outside of the field and near of the moon every 30 min during observations, this takes 3 min on average: 1 min for centering the star field, 1 min, recording, 1 min to recenter the moon. This is very important because calibration with these stars contribute effectively to correct the effect generated by the atmosphere (air-mass, extinction, seeing…). In the Fig. 4 we present as an example a star field used to calibrate photometric measurements of flash detected on April 14, a short video was recorded 5 min before the start of the observation session and 10 min before the flash detection (see Fig. 4). A visual magnitude of 9.4 ±0.2 and 7.7 ± 0.2 are found for respectively the flash 1 and flash 2. The Pogson magnitude relation is used to calculate the energy received at Earth throughout each exposure time which allows us to reconstruct the total visible light energy on the Moon, the star Vega is used as the calibration star (for more photometry details, see Suggs et al. (2014); Bouley et al. (2012) and Madiedo et al. (2013)), the light curve of each flash is shown in the Fig. 3.

2.3 Interpretations

During analysis, lunar impact flashs can be confused with specular reflection from artificial debris in terrestrial orbits, electronic noise or cosmic rays hitting the sensor of the camera. Impact flashes (specifically one frame flash Suggs et al. 2014; Suggs and Moser 2013) must be confirmed by at least two different observatories to exclude other phenomena. It is important to note that these false detections are either a single frame (cosmic ray flashes and electronic noise) or they show motion across the field of view (orbital debris sunglints; Suggs et al. 2014; Suggs and Moser 2013). However, we note that the observed events appear at least in two video full-frames and show brightness changes that are typical of impact flashes. More importantly, the values of magnitudes and duration are consistent with the fact that brighter flashes have often longer durations and the values plot slightly above the trend (see Fig. 5) established from a catalogue of 54 impact flashes compiled by Bouley et al. (2012).

Within this framework, the observations may be interpreted following the sequence of impact flash evolutions. In this first phase, the shock wave vaporizes the regolith of the lunar surface (and the meteoroid) and part of the vapor plume is ionized (plasma phase). Initially, the plume is optically thick and observation of early development of the plume from light emission is probably difficult (Swift et al. 2011). The plasma phase expansion is

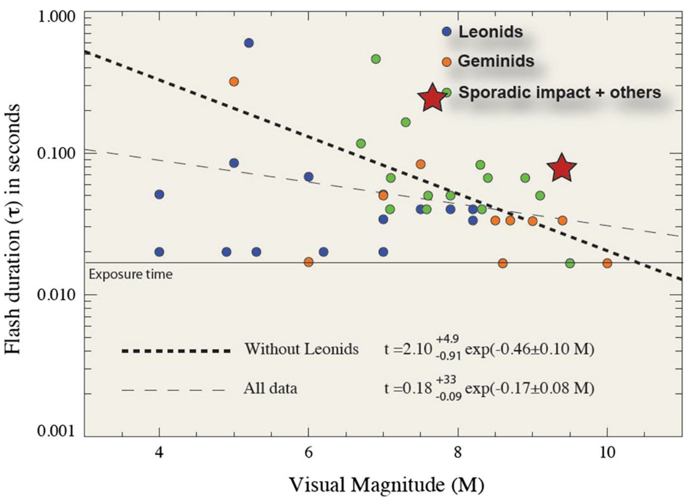

Fig. 5 Duration versus magnitude plot (Bouley et al. 2012) with the two new flashes detected by Moroccan telescopes appearing as *red stars*. (Color figure online)

predicted to be less than 1 ms (Artemieva et al. 2001) and would anyway require higher frame rate to be distinguished from the subsequent phases of cooling. The plume continues to expand and becomes optically thin, and the radiative surface area increases until it reaches its maximum (see for instance the 2nd frame of flash F2 on Fig. 3). The cooling phase of the plume would lead to condensation of liquid droplets and is characterized by a progressive decrease of thermal emissions that would correspond for instance to the 3rd, 4th and 5th frames of the flash 2. The duration of this phase is much longer than the phase of plasma expansion. It is therefore likely that ground-base observations record the thermal emission associated with the cooling and expansion of a cloud of silicate liquid droplets (see for instance 2nd, 3rd, 4th and the 5th zoomed images of the Flash F2 in Fig. 3). Radiation approximated by of a cloud composed of cooling melt droplets assumed to be well represented as black body emitting initially at the vapor/liquid phase transition temperature produce radiation during a time period comparable to the observations (Bouley et al. 2012). Radiation would eventually peak in the near-infrared domain following subsequent cooling to ambient surface temperature. Observation of this phase would be possible using near-infrared cameras but are yet to be reported (Melosh et al. 1993; Bouley et al. 2012).

The inferred photometric parameters of each flash are given in Table 2. Following previous authors (see Rubio et al. 2000; Ortiz et al. 2006; Suggs et al. 2014; Madiedo et al. 2009, 2013; Bellot Rubio et al. 2000; Suggs et al. 2008) the kinetic energy of meteoroids is directly obtained by converting visible light energy on the Moon (kinetic energy = luminous energy/luminous efficiency). Assuming a luminous efficiency factor equal to $\eta = 1.5 \times 10^{-3}$, the kinetic energy obtained is $(3.8 \pm 0.4) \times 10^7$ J for impactor 1 (flash1) and $(23.1 \pm 0.6) \times 10^7$ J for impactor 2 (flash 2). The mass of the impactor is then inferred from its kinetic energy, with an hypothesis on the velocity. Considering a speed of $16\,\mathrm{km\,s^{-1}}$ typical for sporadic impactor speed on the Moon according to the statistics of a large meteoroid orbit database (Steel 1996; Ivanov 2001), the meteoroids masses are about 0.3 ± 0.05 and 1.8 ± 0.3 kg, respectively for the flash 1 and 2. Correspond meteoroids sizes are 7–8 and 14–15 cm for an assumed density of $1500\,\mathrm{kg/m^3}$ for the projectile. The diameter of the impact crater may be estimated using the simplified Gault's formula (Gault et al. 1974) that only requires kinetic energy as the input parameter for the impactor and not specifically its mass and speed. According to this formula, the meteoroids would have produce craters of about 2.6 ± 0.3 and 4.4 ± 0.3 m in diameter (rim-to-rim diameters) for

Table 2 Characteristics of lunar impact flashes

	Flash 1	Flash 2
Duration (ms)	80	240
Estimated Peak magnitude	9.4 ± 0.2	7.7 ± 0.2
Luminous Energy of impact (in visible) (J)	$(5.7 \pm 0.6) \times 10^4$	$(34.1 \pm 8.1) \times 10^4$
Kinetic Energy of impactor (J)	$(3.8 \pm 0.4) \times 10^7$	$(23.1 \pm 5.9) \times 10^7$
Estimated mass of impactor (kg)	0.3 ± 0.05	1.8 ± 0.3
Estimated diameter of impactor (cm)	7–8	14–15
Estimated crater diameter (m)	2.6 ± 0.3	4.4 ± 0.3
Impact coordinates	08.15° ± 0.15°S 59.1° ± 0.15°E	26.81° ± 0.15°N 09.10° ± 0.15°W

Calculated by assuming a meteoroid speed of $16\,\mathrm{km\,s^{-1}}$ and luminous efficiency 1.5×10^{-3}

Table 3 Size of craters corresponds to impact flashes 1 and 2 calculated by Gault's law for different densities of projectile (*Htm* Halley-type meteoroids, *Jfs* Jupiter-family sporadics, *As* asteroidal meteoroids) and target

Lunar density (g/cm^3)	Meteoroids density (g/cm^3)	Diameter 1 (m)	Diameter 2 (m)
2.2	1.5 (Htm)	2.59	4.43
	3.1 (Jfs)	2.92	5.00
	4.2 (As)	3.07	5.27
2.7	1.5 (Htm)	2.33	4.00
	3.1 (Jfs)	2.63	4.52
	4.2 (As)	2.77	4.75
3.1	1.5 (Htm)	2.18	3.73
	3.1 (Jfs)	2.46	4.22
	4.2 (As)	2.59	4.43

flash 1 and 2, respectively, for an assumed density of 1500 kg/m^3 for the projectile and a target density of 2200 kg/m^3 corresponding to recent estimated of the density of the lunar crust and a surface porosity 30 % (Huang and Wieczorek 2012). The Table 3 shows the sizes found for different densities of meteoroids and lunar crust. Note that the estimation of the range of diameter values is very useful for the search of impact crater in the LROC images or other future orbiter camera. The calculation of projectile masses and sizes are accurate if detections may be associated with a meteor shower, because the impact speed is better constrained in this case. This will help to constraints upon the size of the largest meteoroids within a cometary or asteroidal steam. And this is very important because the presence of meter-sized meteoroids in the stream is very difficult to be betrayed by direct telescopic observation. The manner in which such observations could be made have been outlined, for example, by Baggaly (1977). And an attempt was conducted during the Perseid shower of 2004 (Beech et al. 2004) but no distinct detection of any large exo-atmosphere Perseid meteoroids was made.

The uncertainties mentioned in the last paragraph and in Table 2 are associated with the uncertainty of the photometric magnitude only and does not take into account the uncertainty on speed and the luminous efficiency. The luminous efficiency concept plays a part very important in calculations, based on numerical simulations and analysis of impact flashes on the moon its value was reached between $1{-}2\times10^{-3}$ (Bellot Rubio et al. 2000; Artemieva et al. 2001; Bellot Rubio et al. 2000; Artemieva et al. 2000), and a nominal value of 2×10^{-3} was determined from Leonid impact flashes $(72\,\mathrm{km\,s^{-1}})$, whereas at $16\,\mathrm{km\,s^{-1}}$, a much smaller value has ben expected (Ortiz et al. 2000, 2006). Despite this, a value of 2×10^{-3} has been used in more recent detections associated with sporadic events with speed of $17\,\mathrm{km\,s^{-1}}$ (Ortiz et al. 2006; Madiedo et al. 2013). In Swift et al. (2011), the luminous efficiency has been characterized for objects of different velocities, based on their results, the expression for luminous efficiency as a function of speed can be written as: $\eta = 1.5\times10^{-3}\exp(-9.3/v^2)$ (where v is given in km/s), it has also been reported in this work that the luminous efficiency has an extremely large variation with velocity in the range of 6 to $15\,\mathrm{km\,s^{-1}}$ but a necessarily small variation with velocity in range of 20 to $70\,\mathrm{km\,s^{-1}}$. In order to examine separately the effect of the uncertainties on velocity and the luminous efficiency on the deduced parameters, we present in the Fig. 6 the kinetic energy and projectile mass (corresponds to the second flash) for different speeds and luminous

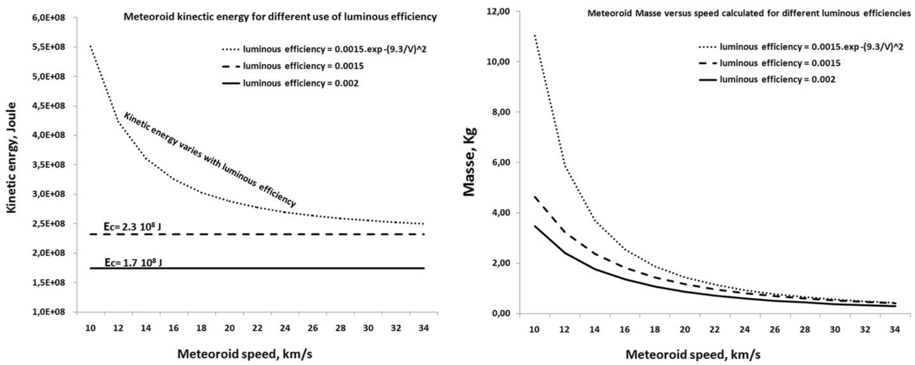

Fig. 6 *Left* kinetic energy corresponding to the flash 2 obtained by converting visible light energy by the use of different luminous efficiency factor. *Right* meteoroid masses corresponding to the flash 2 versus speed calculated for different luminous efficiencies

efficiencies. The range of speeds is considered between 10 and 34 $\mathrm{km\,s^{-1}}$ (adequate for sporadic meteoroids). The kinetic energy of the impactor changes from 2.3×10^8 to 1.7×10^8J, if we consider a luminous efficiency of 2×10^{-3} instead of 1.5×10^{-3}, in this case the mass of the meteoroid is 1.36 kg rather than 1.81 kg when considering a speed of 16 $\mathrm{km\,s^{-1}}$. Using the velocity-dependent luminous efficiency from Swift et al. (2011), the value of this factor varies between 6.3×10^{-4} and 1.4×10^{-3}, leading to a kinetic energy between 5.5×10^8 and 2.5×10^8 J (see Fig. 6). The mass of the impactor at a speed of 16 $\mathrm{km\,s^{-1}}$ is 2.5 kg in this case.

3 Accurate Positioning on the Moon's Surface

3.1 Methods

Different strategies may be conceived in order to achieve a precise positioning of the flash at the surface of the Moon. As flashes are observed on the non-illuminated fraction of the lunar disk, video frames are generally featureless, precluding the direct identification of lunar surface features. Precise astrometry would be necessary in this case and would require modeling of the lunar configuration at the time of observation and of the geometric distortion of the optical system. However, when observations are performed soon after or before the new Moon, which is the case for the two flashes presented here, the Earthshine is luminous enough to develop an alternative approach.

It is of note that large-scale lunar features, such as mare or major impact craters may be identified on the recorded video frames before and after the occurrence of the two impact flashes. As a large number of frames are recorded, it is especially easy to add together a large number of images in order to increase the signal to noise ratio and produce an optimal image of the non-illuminated fraction of the Moon. Increasing the number of images will at some point decrease the resolution due to changes in observation conditions or atmospheric turbulence. It has been found empirically that no significant improvement are attained above one hundred images. Due to the non-perfect tracking of the lunar movement, slight changes in the observation geometry are possible when stacking the images. Images were

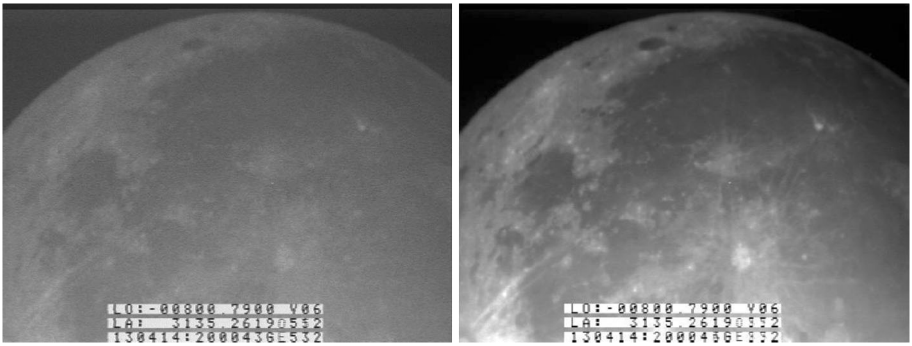

Fig. 7 *Left* Example of a typical video frame (contrast is enhanced to maximum). *Right* Stack of 79 video frames illustrating the benefit of stacking images for the identification of surface features in the Moon that are illuminated only by the Earthshine

therefore registered to the first image of the stack (base frame). The sub-pixel shift of each image relative to the first frame (base frame) was determined by fitting the correlation peak obtained in the Fourier space to a 2-dimensional Gaussian following Schaum and McHugh (1996) and Baratoux et al. (2001). This approach is efficient when the expected shift between two images is a small fraction of the size of the image (Schaum and McHugh 1996), which is the case here, and has been applied in a variety of contexts such as the detection of glaciers of landslides movements (Casson et al. 2003; Berthier et al. 2005). Smaller-scale lunar features are easily identified after application of the procedure (Fig. 7). The accuracy of the positioning would be limited by the size of the flash, which is usually spread over several pixels. To increase further the positioning, the signal of the flash is fitted to a 2-dimensional Gaussian firstly for each frame (previously shifted to the base image) where the flash is present and to the stacked frames.

The barycenter of the flash is given as the rounded to the nearest integer of the average centers of the 2-dimensional Gaussian functions. An image with the flash represented as a single illuminated pixel is then generated. We note that a possible mismatch may remain between the barycenter of radiation and the actual position of the impact, which is of critical importance for determining the position and of seismic source, and also for the possible search of the associated new impact structure on LROC images. This possible shift would result from the viewing angle of the expanding vapor plume and is maximum close to the limb, where image resolution also strongly decreases. Such issue may be resolved by using stereoscopic observations from observations made with distant telescopes $\geq$50 km. The two flashes reported in this study are optimally situated on central region of the lunar disk and this effect is neglected here.

Once the optimal image of the non-illuminated fraction of the Moon has been produced, tie-points are manually selected with an image of the full-Moon. A ground-based image of the Moon (4304 $\times$ 4307 pixels) obtained from telescopic observations was selected for this purpose. The accuracy of the positioning would be limited by the size of the flash, which is usually spread over several pixels. These ties points are then used to perform a rotation, change of scale and translation transformation of the stacked frames and of the frames on which the flash occurs (converted into a single-pixel flash) into this reference geometry. This operation allows us to identify the faintest resolvable features in the vicinity of the impact flash and to superpose directly the frames with the flash on the reference image of the Moon, where surface features are then easily distinguished. The position of the flash may be then represented over high-resolution images available from the Google Moon Web service, and selenographic coordinates may be also derived in this way. The estimate of the positioning accuracy is calculated assuming that the center of flash may be localized with an accuracy around 1 pixel, which corresponds to 5 km on the central part of the disk.

3.2 Application of the Method

The spread of the each flash over several pixels and the Gaussian function which is adjusted to the stacked frames are illustrated on Fig. 8. The stacked frames corresponding to each flash is represented. Firstly the same procedure was applied separately on all video frames where the flashes is observed, and secondly on the stack of these video frames. A successful adjustment to a gaussian function has been done for only 2 video frames for the flash 1 and 4 video frames for the flash 2. The estimated pixel coordinates for each video frame and for the stacked frames are given in Table 4. Differences in positioning remain at

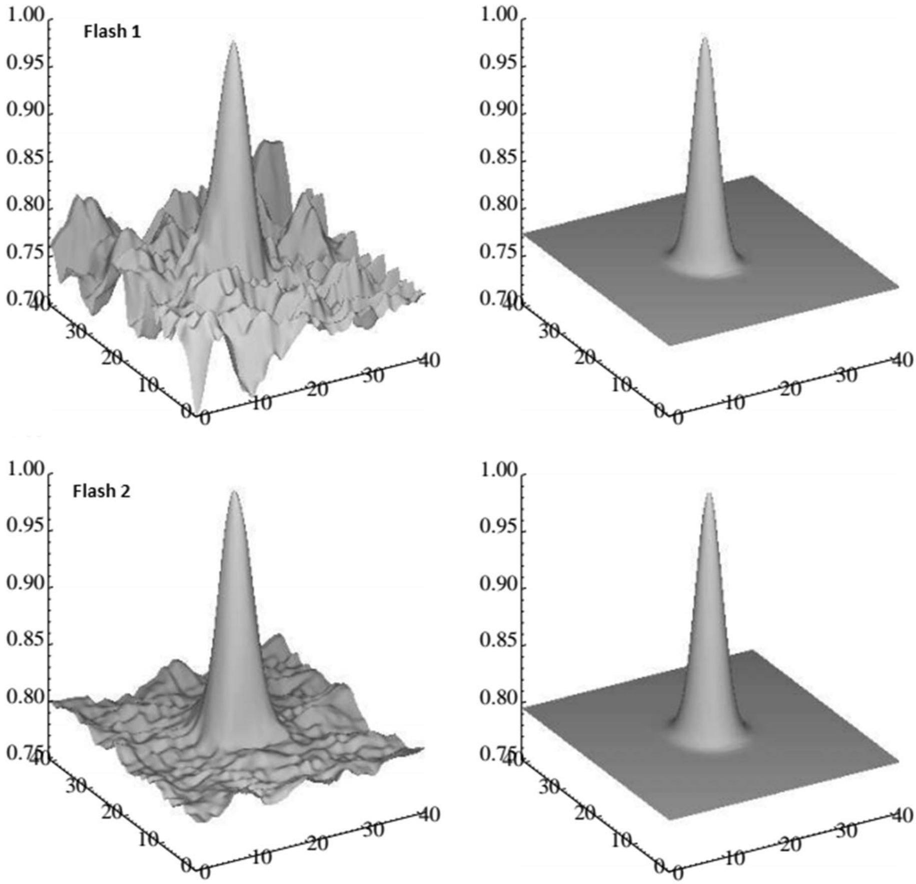

Fig. 8 *Left* shade surface representation of the intensity of the peak corresponding to the flash 1 and 2. *Right* corresponding Gaussian fit of the peak used for the sub-pixel determination of the flash position at the surface of the Moon

Table 4 Pixel coordinates on the video frames of the lunar impact flashes 1 and 2

Video frame reference	Sample	Line
Flash1		
sf00030	100.51	195.22
sf00031	100.11	196.35
Stacked frames	100.44	195.56
Flash 2		
sf00107	540.56	23.33
sf00108	540.48	23.33
sf00109	540.61	23.04
sf00110	541.23	23.22
Stacked frames	540.57	23.26

the sub-pixel level. This confirms that the uncertainly on the position of the flash is better then one pixel.

The Figs. 9 and 10 represents the video frames where each flash reaches its maximum intensity and the stacked images on which the position of flashes, as given by the center of the gaussian function, is represented by a single illuminated pixel (in red). This images is then warped to the reference image of the Moon. A final comparison with this pixel positions on the reference image with high-resolution images of the Moon allows us to determine precisely the position of the flash (Figs. 11 and 12). The coordinates of the first flash are $08.15^\circ \pm 0.15^\circ$S $59.1^\circ \pm 0.15^\circ$E and those of the second flash are $26.83^\circ \pm 0.15^\circ$N $09.16^\circ \pm 0.15^\circ$W, the uncertainty correspond to 5 km.

3.3 Implications for Lunar Seismology

As previously demonstrated by Yamada et al. (2011), the location of impact flashes greatly improves the determination of the crustal structure of the Moon by future lunar seismometers. The space/time location of the impact allows to reduce the uncertainty on the seismic source location. In particular, the timing of the impact is determined to better than 0.05 s which is the usual sampling rate of broadband seismometers, and the depth of the seismic source is known. Table 5 presents body wave travel time errors computed in VPREMOON model (Garcia et al. 2011) for a 5 km epicentral distance uncertainty for various phases at different epicentral distances. For such a small distance uncertainty, the error induced on the travel times is a factor 6 smaller than the average 3 s travel time reading error ascribed to body wave phases detected by ALSEP Apollo seismological network (Gagnepain-Beyneix et al. 2006). So, the impact flash detection decreases strongly the seismic source location uncertainties. Thus allowing a precise determination of the internal structure from body wave travel times. In addition, the estimate of source energy allows to infer intrinsic attenuation of seismic waves and its variations. Because impacts are more easily detected by seismometers at short epicentral distances these combined seismic wave/flashes observations would strongly constrain the internal structure of the crust.

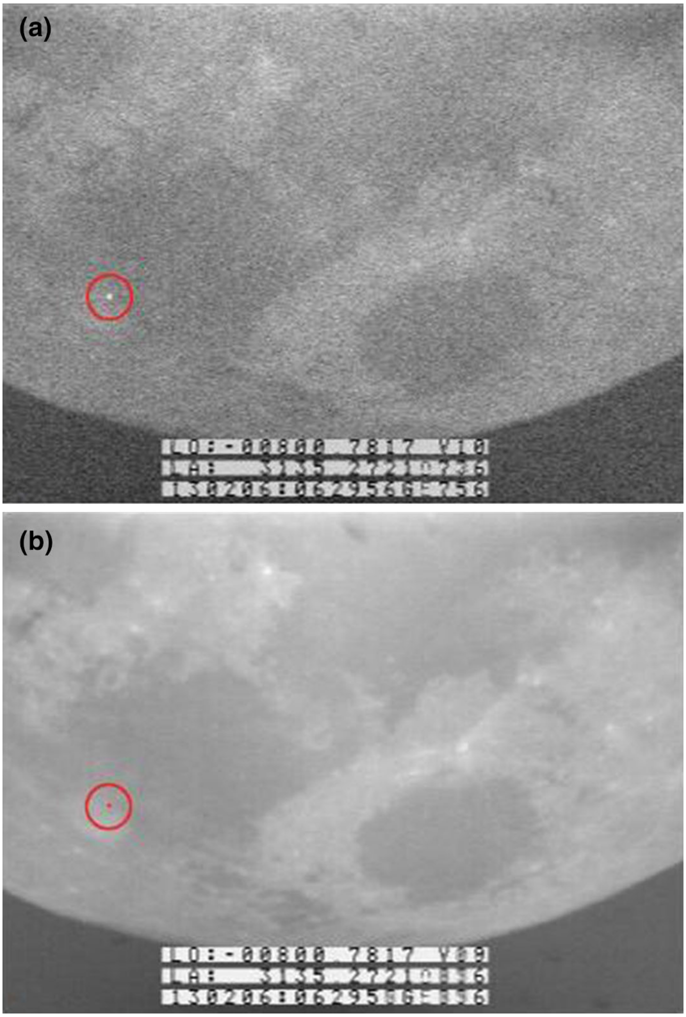

Fig. 9 **a** Video frame of the flash recorded on February 6, 2013 corresponding to the maximum of intensity. The flash is spread over several pixels (**b**). The position of the flash given as a single illuminated pixel is represented on the stacked video frames

4 ILIAD Network of Observatories

Since 2005, U.S. Marshall Space Flight Center has detected more than 300 flashes (Suggs et al. 2014). 240 of these detections were done from 2005 to 2011 (Only 126 with necessarily quality for good analysis(Suggs et al. 2014, 2008, 2011a, b), because 294 nights of observations was performed among 600 nights scheduled and both the conditions of observation of the Moon (Moon phases appropriate with lunar flash observations) and the weather was favorable at the peak of major meteor showers during this period (Suggs et al. 2011a). Today, they have two observation centers (Alabama and New Mexico), which allow them to observe during $\sim$1 h/day when the lunar phase is around 0.1 and $\sim$6 h/day

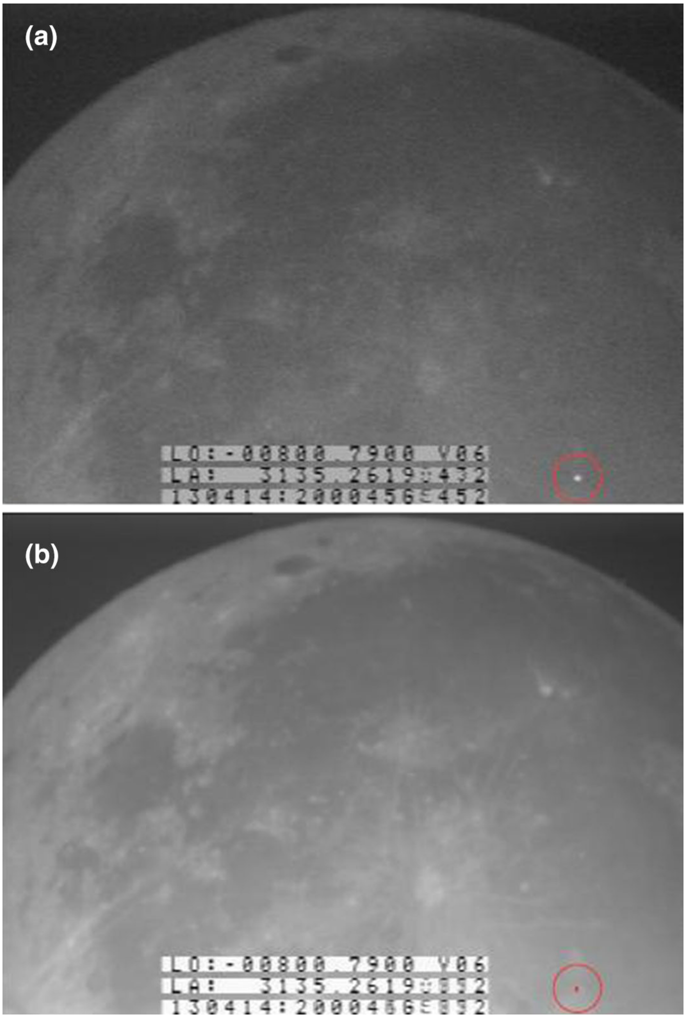

Fig. 10 **a** Video frame of the flash recorded on April 14, 2013 corresponding to the maximum of intensity. The flash is spread over several pixels (**b**). The position of the flash given as a single illuminated pixel is represented on the stacked video frames

during a first or last quarter. Similarly, A project named MIDAS, which is the acronym for Moon Impacts Detection and Analysis System was performed in 2009 by a Spanish team from the University of Seville and Astrophysics Institute of Andalusia (Madiedo et al. 2009, 2013). According to statistics from NASA (Suggs et al. 2014, 2011a), there are on average 2–4 flashes/h to detect during meteors shower and 1 flash/2 h in the case of a sporadic impacts monitoring based on 752 h of lunar video observations performed over a period of 5 years. From Brown et al. (2002), a meteoroid of 10 cm should fall on the visible part of the Moon every day. As shown by Bouley et al. (2012), a meteoroid of this size should produce a bright lunar flash with a peak V magnitude between 5 and 8 depending on velocity and density of the meteoroid.

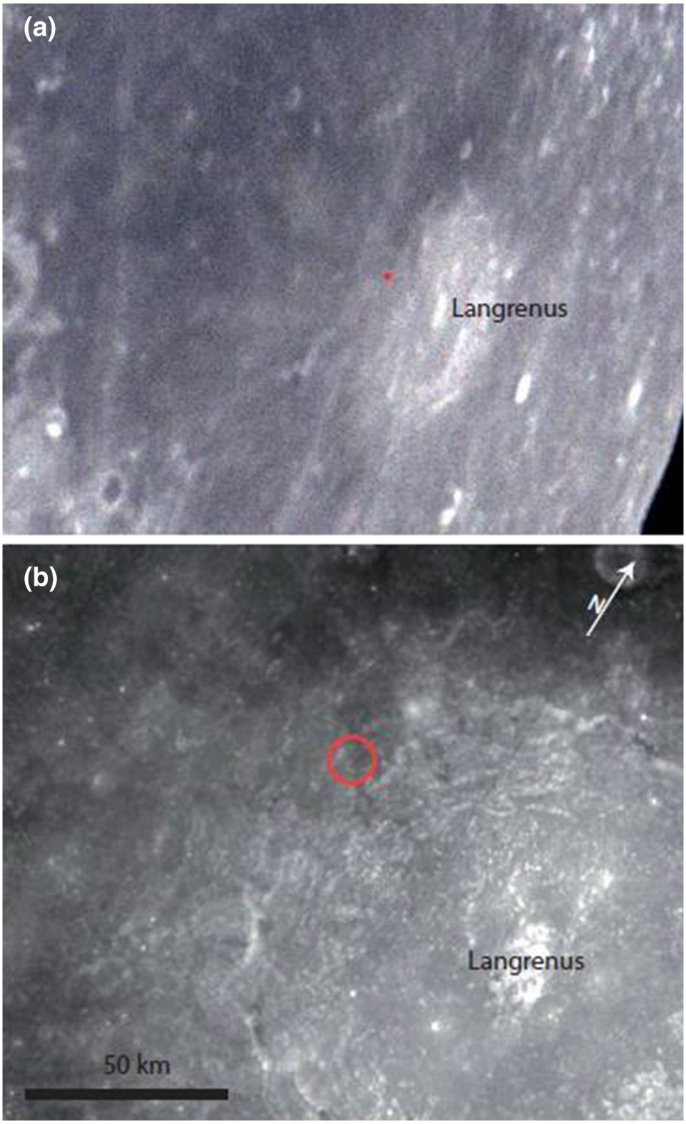

Fig. 11 **a** Localization of the flash recorded on February 6, 2013 on a reference image of the Moon. The video frame has been warped into the geometry of the reference image of the Moon. **b** Close-up view of the possible position of the impact crater associated with the lunar flash. Background is given from SELENE images available from the Google Moon website

To increase the number of detections, it is crucial to increase the observation time by monitoring the Moon at different longitudes (see Fig. 2). This study shows that mid-sized telescope with available time around the world may significantly contribute to this area of research. Figure 13 illustrates how the setting of observatories for lunar flashes in more than a dozen countries will allow to observe almost 24 h/day for a lunar quarter phase and 10 h/day for a 0.1 lunar phase. For this purpose, observatories in France, Morocco and

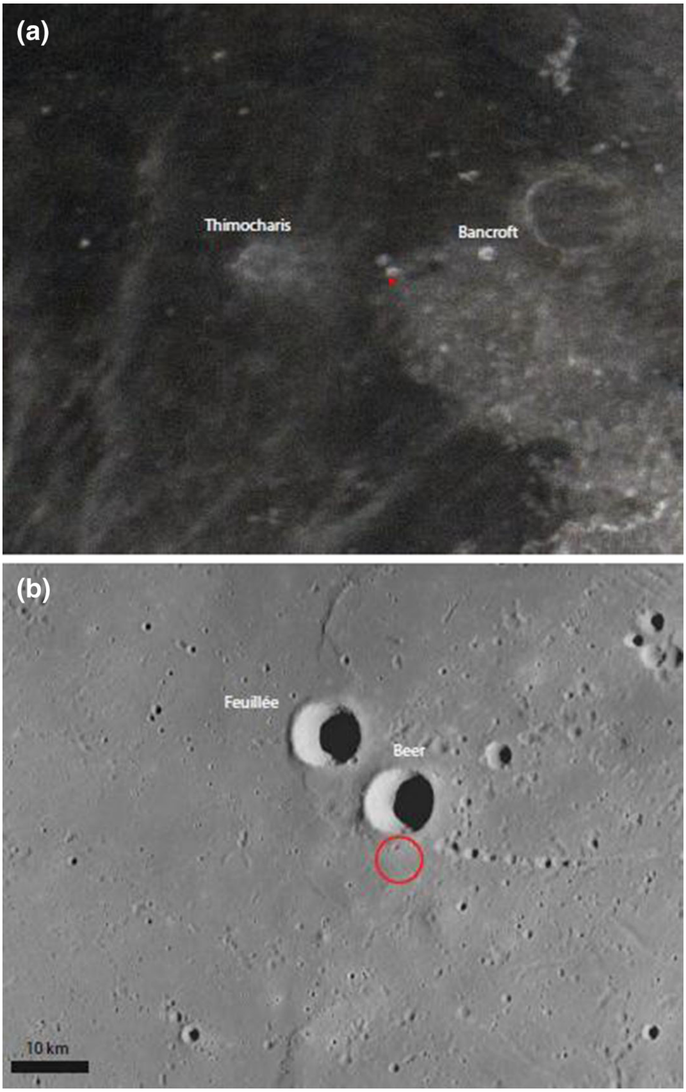

Fig. 12 **a** Localization of the flash recorded on April 14, 2013 on a reference image of the Moon. The video frame has been warped into the geometry of the reference image of the Moon. **b** Close-up view of the possible position of the impact crater associated with the lunar flash. Background is given from SELENE images available from the Google Moon website

Mongolia have started to developed a informal network of lunar impact flashes monitoring stations. The network has been named ILIAD, the acronym standing for Lunar Impacts Astronomical Detection. The ILIAD network has also the objective to develop specific techniques of observations and data processing for improving the localization of the flash, which is critical for future seismological applications and for identification of new impact structure on LROC images or other future lunar orbiter cameras (Fig. 1).

Table 5 Seismic body wave travel time uncertainties due to 5 km impact mislocation, as a function of seismic phase and epicentral distance (in degrees)

Body waves	10° (s)	30° (s)	60° (s)	90° (s)	120° (s)	150° (s)	180° (s)
P	0.65	0.62	0.52	0.42	0.3	0.15	–
S	1.12	1	0.92	0.72	0.42	0.25	–
ScS	0.03	0.04	0.15	0.2	0.25	0.3	–
PKP	–	–	–	–	0.13	0.11	0.03

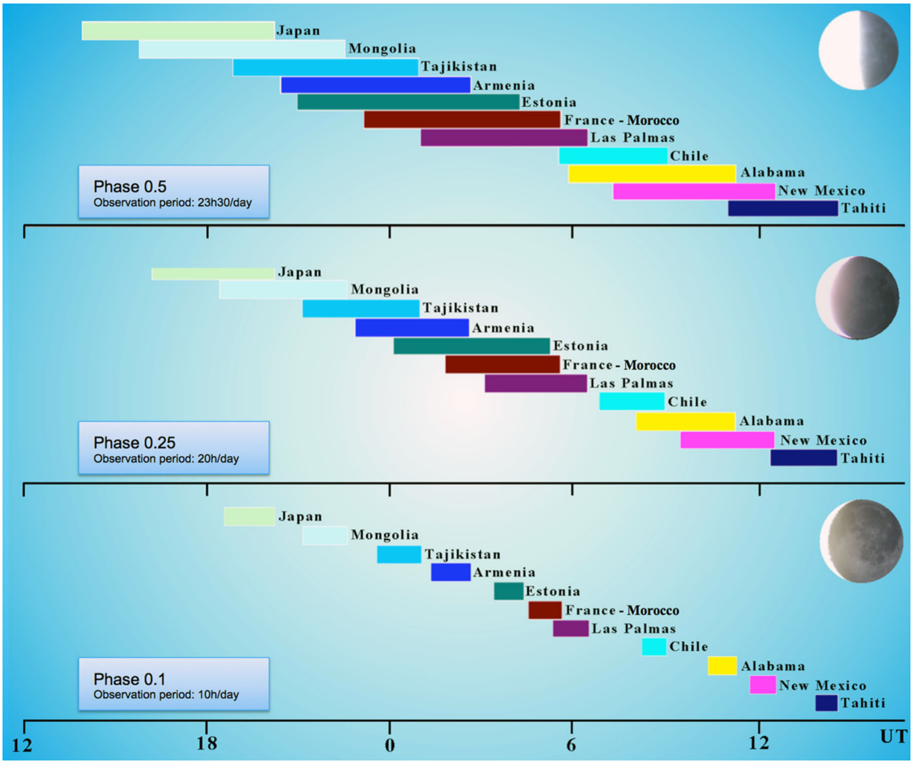

Fig. 13 Installing observatories for lunar flashes in more than a dozen countries.This Figure shows that such collaborations will allow to observe almost 24 h/day for a lunar quarter phase and 10 h/day for a 0.1 lunar phase

5 Conclusion

The characteristics of the two first flashes detected by AGM observatory in Morocco have been reported here. In addition to provide intensity and duration of the flash, and estimates of the mass of the meteoroids, flash positions are reported using a new technique that does not require the knowledge of observation geometry, and is only based on the identification of lunar surface features illuminated by the Earthshine. This approach is currently limited to the observations near the new Moon, when the Earthshine is more intense, but may be applied to a wider range of conditions of observations if more sensitive sensors become available. Accuracy on flash positioning at 5 km levels are reported here. This effort goes in the right direction for seismological applications but accuracy needs to be improved further (to about 1 km) to produce useful observations for lunar seismology. Development of larger sensors (with a larger number of pixels) would allow to increase further the positioning accuracy. High-precision positioning is also important as it will offer the possibility to compare new and ancient images of the Moon and look for the impact structure associated with the lunar flash. Such an observation would allow for the first time a direct estimate of the partitioning between the amount of the initial kinetic energy that is partitioned into mechanical and radiative/thermal energy.

As mentioned, the observation of lunar-meteoroids impact flashes is motivated in the context of projects for future lunar seismological networks, the exploration of the lunar atmosphere mission, and the search for new impact structures on the lunar surface. Presently, the only dataset of lunar meteoroids impact with the quality needed for meaningful work on this subject is composed of only 300 flashes (not all with considerable quality). To take advantage of the expected objectives in this area of research, more permanent and automated monitoring stations must exist in other countries in addition to those in North America and Spain. We therefore call for the development of an international project (ILIAD—international lunar impacts astronomical detection) with the objective to develop lunar impact flashes monitoring programs in several stations around the globe.

Acknowledgments The authors would like to thank the Partenariat Hubert Curien/Volubilis Program (PHC24675QJ, Impact rate in the Earth-Moon System), which provided financial support for the collaboration between Morocco and France. The Institut National des Sciences de l'Univers and the Observatoire Midi-Pyrénées are also acknowledged for financial support. We are grateful to the Mr. Hila Omar and its company Atlas Golf Marrakech for putting at our disposal the equipments of their observatory.

References

N.A. Artemieva, V.V. Shuvalov, I.A. Trubetskaya, Lunar Leonid meteors numerical simulations. Lunar Planet. Sci. XXXI, Abstract 1402 (2000)

N.A. Artemieva, I.B. Kosarev, I.V. Nemtchinov, I.A. Trubetskaya, V.V. Shuvalov, Light flashes caused by Leonid meteoroid impacts on the lunar surface. Sol. Syst. Res. **35**, 177–180 (2001)

W.J. Baggaly, The possibility of the detection of meteor streams in interplanetary space. Observatory **97**, 123–129 (1977)

D. Baratoux, C. Delacourt, P. Allemand, Digital elevation models derived from viking images :method and comparison to mola data. J. Geophys. Res. **106**(12), 32,927–32,941 (2001)

D. Baratoux, M.J. Toplis, M. Monnereau, V. Sautter, The petrological expression of early Mars vol- canism. J. Geophys. Res. **118**, 59–64 (2013). doi:10.1029/2012JE004234

M. Beech, I. Alison, P. Brown, A telescopic search for large Perseid meteoroids. Mon. Not. R. Astron. Soc. **348**, 13951400 (2004). doi:10.1111/j.1365-2966.2004.07462.x

L.R. Bellot Rubio, J.L. Ortiz, P.V. Sada, Observation and interpretation of meteoroid impact flashes on the Moon. Earth Moon Planets **8283**, 575598 (2000b)

E. Berthier, H. Vadon, D. Baratous, Y. Arnaud, C. Vincente, K.L. Feigl, F. Rmy, B. Legresy, Surface motion of mountain glaciers derived from satellite optical imagery. Remote Sens. Environ. **95**, 14–28 (2005)

J.P. Bibring, Y. Langevin, J.F. Mustard, F. Poulet, R. Arvidson, A. Gendrin, B. Gondet, N. Mangold, P. Pinet, F. Forget, Global mineralogical and aqueous Mars history derived from OMEGA/Mars express data. Science **312**, 400–404 (2006). doi:10.1126/science.1122659

S. Bouley, D. Baratoux, J. Vaubaillon, A. Mocquet, M. Le Feuvre, F. Colas, Z. Benkhaldoun, A. Daassou, M. Sabil, P. Lognonne, Power and duration of impact flashes on the Moon: implication for the cause of radiation. Icarus **218**, 115–124 (2012). doi:10.1016/j.icarus.2011.11.028

P. Brown, R.E. Spalding, D.O. ReVelle, E. Tagliaferri, S.P. Worden, The flux of small near-Earth objects colliding with the Earth. Nature **420**, 294–296 (2002)

B. Casson, C. Delacourt, D. Baratoux, P. Allemand, 17 years of la clapi'ere landslide evolution analysed from aerial ortho-rectified photographs. Eng. Geol. **68**, 123–139 (2003)

R. Clark, H. Melosh, The detectability of lunar impacts in the near infrared. Masters thesis, The University of Arizona, Department of Planetary Sciences, 1996

W.J. Cooke, R.M. Suggs, R.J. Suggs, W.R. Swift, N.P. Hollon, Rate and distribution of kilogram lunar impactors. In *38 lunar and planetary science conference* (2007), p. 1986

B. Cudnik, *Lunar Meteorid Impacts and How to Observe Them* (Springer, Berlin, 2009)

S.S. Davis, An analytical model for a transient vapor plume on the Moon. Icarus **202**, 383–392 (2009). doi:10.1016/j.icarus.2009.03.019

J. Gagnepain-Beyneix, P. Lognonne, H. Chenet, D. Lombardi, T. Spohn, A seismic model of the lunar mantle and constraints on temperature and mineralogy. Phys. Earth Planet. Inter. **159**, 140–166 (2006). doi:10.1016/j.pepi.2006.05.009

R.F. Garcia, J. Gagnepain-Beyneix, S. Chevrot, P. Lognonne, Very preliminary reference Moon model. Phys. Earth Planet. Inter. **188**, 96–113 (2011). doi:10.1016/j.pepi.2011.06.015

D.E. Gault, R. Greeley, P.H. Schultz, A primer in lunar geology. Moffett Field: NASA Ames Research Center (1974), pp. 137–175

P. Gural, Automated detection of lunar impact flashes. Meteoroid environments workshop. NASA MSFC, Huntsville, Alabama (2007)

W. Hartmann, Martian cratering 8: isochron refinment and the chronology of Mars. Icarus **174**, 294–320 (2005). doi:10.1016/j.icarus.2004.11.023

H. Hiesinger, J.W. Head, U. Wolf, R. Jaumann, G. Neukum, Ages and stratigraphy of lunar mare basalts in Mare Frigoris and other nearside maria based on crater size-frequency distribu- tion measurements. J. Geophys. Res. **115**(E14), 3003 (2010). doi:10.1029/2009JE003380

Q. Huang, M.A. Wieczorek, Density and porosity of the lunar crust from gravity and topography. J. Geophys. Res. **117**, 5003 (2012). doi:10.1029/2012JE004062

B.A. Ivanov, Mars/Moon cratering rate ratio estimates. Sp. Sci. Rev. **96**, 87–104 (2001)

B.A. Ivanov, Earth/Moon impact rate comparison: searching constraints for lunar secondary/primary cratering proportion. Icarus **183**, 504–507 (2006). doi:10.1016/j.icarus.2006.04.004

M. Iye, M. Tanaka, M. Yanagisawa, N. Ebizuka, K. Ohnishi, C. Hirose, N. Asami, Y. Komiyama, H. Furusawa, SuprimeCam observation of sporadic meteors during Perseids 2004. Publ Astron Soc Jpn **59**, 841–855 (2007)

M. Le Feuvre, M.A. Wieczorek, Nonuniform cratering of the terrestrial planets. Icarus **197**, 291–306 (2008). doi:10.1016/j.icarus.2008.04.011

M. Le Feuvre, M.A. Wieczorek, Nonuniform cratering of the Moon and a revised crater chronology of the inner Solar System. Icarus **214**, 1–20 (2011). doi:10.1016/j.icarus.2011.03.010

P. Lognonné, M. Le Feuvre, C.L. Johnson, R.C. Weber, Moon meteoritic seismic hum: steady state prediction. J Geophys Res **114**(E13), E12,003 (2009). doi:10.1029/2008JE003294

J.M. Madiedo, J.L. Ortiz, J.M. Trigo-Rodrguez, N. Moral, J. Cabrera-Cano, A large lunar impact blast on september 11th 2013. Mon. Not. R. Astron. Soc. (2013) doi:10.1093/mnras/stu083

J.M. Madiedo, J.M. Trigo-Rodrguez, J.L. Ortiz, N. Moral, Robotic systems for meteor observing and moon impact flashes detection in Spain. Adv. Astron. (2009) doi:10.1155/2010/167494

S. Marchi, S. Mottola, G. Cremonese, M. Massironi, E. Martellato, A new chronology for the Moon and Mercury. Astron. J. **137**, 4936–4948 (2009). doi:10.1088/0004-6256/137/6/4936

S. Marchi, H.Y. McSween, D.P. Obrien, P. Schenk, M.C. De Sanctis, R. Gaskell, R. Jaumann, S. Mottola, F. Preusker, C.A. Raymond, T. Roatsch, C.T. Russell, The violent collisional history of asteroid 4 Vesta. Science **336**, 690 (2012). doi:10.1126/science.1218757

H.J. Melosh, N.A. Artemjeva, A.P. Golub, I.V. Nemchinov, V.V. Shuvalov, I.A. Trubetskaya, Remote visual detection of impacts on the lunar surface. In *24th lunar and planetary institute science conference abstracts* (1993), pp. 975–976

D. Mimoun, M.A. Wieczorek, L. Alkalai, W.B. Banerdt, D. Baratoux, J.L. Bougeret, S. Bouley, B. Cecconi, H. Falcke, J. Flohrer, R.F. Garcia, R. Grimm, M. Grott, L. Gurvits, R. Jaumann, C.L. Johnson, M. Knapmeyer, N. Kobayashi, A. Konovalenko, D. Lawrence, M.L. Feuvre, P. Lognonne, C. Neal, J. Oberst, N. Olsen, H. Rottgering, T. Spohn, S. Vennerstrom, G. Woan, P. Zarka, Farside explorer: unique science from a mission to the farside of the moon. Exp Astron **33**, 529–585 (2012). doi:10.1007/s10686-011-9252-3

O. Mousis, et al. Instrumental methods for professional and amateur collaborations in planetary astronomy. Exp Astron **38**(1–2), 91–191 (2013). doi:10.1007/s10686-014-9379-0

G. Neukum, R. Jaumann, H. Hoffmann, E. Hauber, J. Head, A. Basilevsky, B. Ivanov, S. Werner, S. van Gasselt, J. Murray, T. McCord, H.C.I. team, Recent and episodic volcanic and glacial activity on mars revealed by the high resolution stereo camera. Nature **432**, 971–979 (2004)

J. Oberst, A. Christou, R. Suggs, D. Moser, I.J. Daubar, A.S. McEwen, M. Burchell, T. Kawamura, H. Hiesinger, K. Wunnemann, R. Wagner, M.S. Robinson, The present-day flux of large meteoroids on the lunar surface—a synthesis of models and observational techniques. Planet. Sp. Sci. **74**, 179–193 (2012)

J.L. Ortiz, P.V. Sada, L.R. Bellot Rubio, F.J. Aceituno, J. Aceituno, P.J. Gutierrez, U. Thiele, Optical detection of meteoroidal impacts on the Moon. Nature **405**, 921–923 (2000)

J.L. Ortiz, F.J. Aceituno, J.A. Quesada, J. Aceituno, M. Fernandez, P. Santos-Sanz, J.M. Trigo- Rodrguez, J. Llorca, F.J. Martn-Torres, P. Montan es-Rodrguez, E. Palle, Detection of spo- radic impact flashes on the Moon: implications for the luminous efficiency of hypervelocity impacts and derived terrestrial impact rates. Icarus **184**, 319–326 (2006). doi:10.1016/j.icarus.2006.05.002

F. Poulet, N. Mangold, B. Platevoet, J.M. Bardintzeff, V. Sautter, J.F. Mustard, J.P. Bibring, P. Pinet, Y. Langevin, B. Gondet, A. Al eon-Toppani, Quantitative compositional analysis of martian mafic regions using the MEx/OMEGA reflectance data. 2. Petrological implications. Icarus **201**, 84–101 (2009). doi:10.1016/j.icarus.2008.12.042

C. Quantin, N. Mangold, W.K. Hartmann, P. Allemand, Possible long-term decline in impact rates. 1. Martian geological data. Icarus **186**, 1–10 (2007). doi:10.1016/j.icarus.2006.07.008

L.R. B. Rubio, J.L. Ortiz, P.V. Sada, Luminous efficiency in hypervelocity impacts from the 1999 lunar Leonids. Astrophys. J. **542**, L65–L68 (2000a). doi:10.1086/312914

A. Schaum, M. McHugh, Analytical methods of image registration : displacement estimation and resampling. Tech. Rep. NRL Report 9298, Image registration and correlation (1996)

D. Steel, Meteoroid orbits. Sp. Sci. Rev. **78**, 507–553 (1996)

R.M. Suggs, W.J. Cooke, H.M. Koehler, R.J. Suggs, D.E. Moser, W.R. Swift, Lunar meteoroid impact observations and the flux of kilogram-sized meteoroids. In *Proceedings of the meteoroids 2010 conference, NASA CP-2011-216469* (2011b), pp. 116–124

R. Suggs, D. Moser, Lunar meteoroid impact monitoring for LADEE. Lunar meteoroid impacts and LADEE mission workshop (2013)

R.M. Suggs, D.E. Moser, W.J. Cooke, R.J. Suggs, The flux of kilogram-sized meteoroids from lunar impact monitoring. Icarus **238**, 23–36 (2014). doi:10.1016/j.icarus.2014.04.032

R.J. Suggs, R.M. Suggs, D.E. Moser, D. Blaauw, The Flux of kilogram-sized Meteoroids from lunar impact monitoring. NASA Meteor video observations and analysis workshop (2011a)

R.M. Suggs, W.J. Cooke, R.J. Suggs, W.R. Swift, N. Hollon, The NASA lunar impact monitoring program. Earth Moon Planets **102**, 293–298 (2008). doi:10.1007/s11038-007-9184-0

W.R. Swift, D.E. Moser, R.M. Suggs, W.J. Cooke, An exponential luminous efficiency mode for hypervelocity impact into lunar regolith. In *Proceedings of the meteoroids 2010 conference, NASA CP-2011-216469* (2011), pp. 116–124

J. Vaucher, D. Baratoux, N. Mangold, P. Pinet, K. Kurita, M. Gregoire, The volcanic history of central Elysium Planitia: Implications for martian magmatism. Icarus **204**, 418–442 (2009). doi:10.1016/j.icarus.2009.06.032

R. Yamada, R.F. Garcia, P. Lognonne, M.L. Feuvre, M. Calvet, J. Gagnepain-Beyneix, Optimisation of seismic network design: application to a geophysical international lunar network. Planet. Sp. Sci. **59**, 343–354 (2011). doi:10.1016/j.pss.2010.12.007

M. Yanagisawa, N. Kisaichi, Lightcurves of 1999 Leonid impact flashes on the Moon. Icarus **159**, 31–38 (2002)

M. Yanagisawa, K. Ohnishi, Y. Takamura, H. Masuda, Y. Sakai, M. Ida, M. Adachi, M. Ishida, The first confirmed Perseid lunar impact flash. Icarus **182**, 489–495 (2006). doi:10.1016/j.icarus.2006.01.004